Interferon-α-Induced Endogenous Superantigen: A Model Linking Environment and Autoimmunity

Yves Stauffer,[1,4] Samuel Marguerat,[1,4]
Françoise Meylan,[1,4] Catherine Ucla,[1]
Natalie Sutkowski,[2] Brigitte Huber,[2]
Thierry Pelet,[1] and Bernard Conrad[1,3]
[1]Department of Genetics and Microbiology
University of Geneva Medical School
1211 Geneva 4
Switzerland
[2]Department of Pathology
Tufts University
Boston, Massachusetts 02111

Summary

We earlier proposed that a human endogenous retroviral (HERV) superantigen (SAg) IDDMK$_{1,2}$22 may cause type I diabetes by activating autoreactive T cells. Viral infections and induction of interferon-α (IFN-α) are tightly associated with the onset of autoimmunity. Here we establish a link between viral infections and IFN-α-regulated SAg expression of the polymorphic and defective HERV-K18 provirus. HERV-K18 has three alleles, IDDMK$_{1,2}$22 and two full-length envelope genes, that all encode SAgs. Expression of HERV-K18 SAgs is inducible by IFN-α and this is sufficient to stimulate Vβ7 T cells to levels comparable to transfectants constitutively expressing HERV-K18 SAgs. Endogenous SAgs induced via IFN-α by viral infections is a novel mechanism through which environmental factors may cause disease in genetically susceptible individuals.

Introduction

T cell-mediated autoimmune diseases, such as type I diabetes, are thought to result from activation of autoreactive T cells. Activation of autoreactive T cells may be brought about by viral infections, via conventional presentation of viral peptides and bystander activation or, alternatively, by SAgs (Steinman, 1995). Superantigens are microbial proteins that sequentially bind to MHC class II proteins and the Vβ chain of the T cell receptor and thereby strongly stimulate and expand T cells (Marrack et al., 1993). A dominant pancreatic enrichment of Vβ7 T cells led to the detection of a Vβ7- and Vβ13-specific SAg present in the protein fraction of inflammatory lesions from diabetic patients (Conrad et al., 1994). It turned out to be encoded by the truncated envelope gene of a HERV named IDDMK$_{1,2}$22 (Conrad et al., 1997). Expansion of Vβ7 and Vβ13 T cells in the circulation closely correlates with and precedes the onset of the clinical disease (Luppi et al., 2000). The IDDMK$_{1,2}$22 SAg may therefore drive activation of autoreactive T cells in type I diabetes.

Multiple genes contribute to familial clustering of type I diabetes, the MHC locus being the most important. While genetic factors are necessary, they are per se not sufficient (Tisch and McDevitt, 1996). Environmental factors and particularly viral infections have been proposed to contribute to initiating and/or accelerating autoimmunity (Singh et al., 1998). Several lines of evidence support this. Clear correlations were found between elevated levels of circulating IFN-α and type I diabetes (Chehadeh et al., 2000b). In almost all cases of recent onset diabetes, the pancreatic β cells contained IFN-α and this correlated with overexpression of the INF-α target gene MHC class I (Foulis et al., 1987). IFN-α expression in pancreatic β cells is consistent with persistent viral infections (Chehadeh et al., 2000a). Transgenic β cell-specific expression of type I IFNs caused type I diabetes, and development of the disease depended on the genetic background of the mice (Stewart et al., 1993; Pelegrin et al., 1998). Finally, therapeutic administration of IFN-α provoked type I diabetes in some individuals with genetic risk factors (Beales and Pozzilli, 1999).

HERVs entered the human genome after fortuitous germ line integration of exogenous retroviruses and were subsequently fixed in the general population. They may have been preserved to ensure genome plasticity and this can provide the host with new functions, such as protection from exogenous viruses and fusiogenic activity (Goff, 1996; Stoye and Coffin, 2000). IDDMK$_{1,2}$22 is a member of the HERV-K family, which has been assigned ten proviruses with distinct integration sites to date (Barbulescu et al., 1999). The provirus encoding IDDMK$_{1,2}$22 has not yet been characterized. However, proviruses similar to IDDMK$_{1,2}$22 with integration sites in common with HERV-K18 were described (Tonjes et al., 1999; Hasuike et al., 1999; Barbulescu et al., 1999). A sequence similar to both HERV-K18 and IDDMK$_{1,2}$22 was preliminarily mapped to the CD48 gene on chromosome 1 using DNA from a single individual (Hasuike et al., 1999).

Here we provide a model linking viral infections and autoimmunity via IFN-α-regulated SAg expression. First, we unambiguously identify that the polymorphic and defective HERV-K18 provirus in the CD48 gene has three alleles, one of which corresponds to IDDMK$_{1,2}$22. Second, we analyze the population frequency of the three HERV-K18 alleles. The truncated and full-length HERV-K18 envelope alleles all encode SAgs with identical specificity. The HERV-K18 SAgs are expressed at low or not measurable levels in the absence of induction and are strongly induced by IFN-α with rapid kinetics in peripheral blood lymphocytes (PBL). This is sufficient to stimulate Vβ7 T cells to levels comparable to those obtained with transfectants constitutively expressing the SAg. In contrast, the other known HERV-K proviruses are not IFN-α inducible and are instead constitutively expressed. This provides a novel mechanism for a model linking environmental factors such as viral infections and autoimmunity via IFN-α-regulated endogenous SAgs.

[3]Correspondence: bernard.conrad@medecine.unige.ch
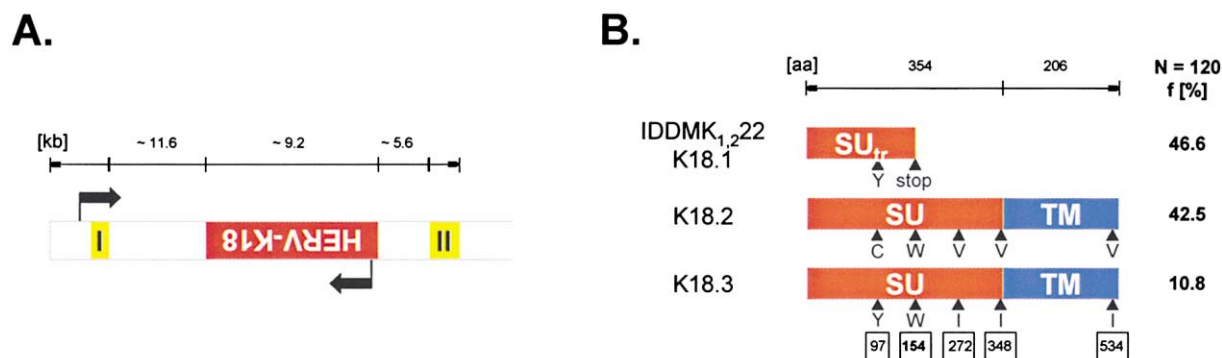[4]These authors contributed equally to this work.

A.

B.

Figure 1. Three Alleles, IDDMK$_{1,2}$22 and Two Full-Length Envelope Genes, Are Encoded by HERV-K18, a Polymorphic and Defective Provirus in the First Intron of the CD48 Gene

(A) HERV-K18 is integrated in an orientation opposite to the transcriptional direction of the CD48 gene. We precisely mapped the provirus and confirmed the uniform presence and orientation of HERV-K18 in the first CD48 intron, on genomic DNA extracted from ∼30 healthy blood donors.

(B) The *env*-LTR region of HERV-K18 is polymorphic. Shown are the deduced amino acid (aa) sequences of the 3 K18 envelope alleles and the respective allele frequencies obtained from 120 different chromosomes of healthy blood donors. The surface (SU) and transmembrane (TM) domains of the envelope protein are indicated by boxes. The position of polymorphic sites and aa changes are specified by arrowheads. Allele K18.1 represents the first described sequence IDDMK$_{1,2}$22 encoding a Vβ7 and -13 specific SAg in the 153 aa of the N-terminal SU region. Alleles 2 and 3 encode full-length envelope proteins that also have SAg function. Two additional variants were found only once. The candidate allele K18.1' differs from K18.1 only in the 3′ LTR. The candidate allele K18.2/3′ is intermediate between alleles 2 and 3. The *gag/pol* coding regions of all three alleles are defective (AF012336).

Results and Discussion

Three Alleles, IDDMK$_{1,2}$22 and Two Full-Length Envelope Genes, Are Encoded by HERV-K18, a Polymorphic and Defective Provirus in the First Intron of the CD48 Gene

We first analyzed the genomic organization and sequence of the provirus within the first CD48 intron in both chromosomes of 60 healthy individuals. This aimed at resolving all ambiguities in sequences similar to IDDMK$_{1,2}$22 and assessing the IDDMK$_{1,2}$22 population frequency. As indicated in Figure 1A, the integration site of the HERV-K18 provirus in the large first CD48 intron was preserved in all individuals tested. The provirus was inserted in the opposite transcriptional direction to CD48. We then determined the envelope sequences because the SAg is encoded within the envelope gene. In fact, the IDDMK$_{1,2}$22 SAg coding sequence was found in 46.6% of chromosomes and was designated allele K18.1 (Figure 1B). Two envelope sequences similar to IDDMK$_{1,2}$22, but without its premature stop codon, were obtained at frequencies of 42.5% (allele K18.2) and 10.8% (allele K18.3). K18.2 is identical to a published sequence (Tonjes et al., 1999) and K18.3 is novel. Two additional variants were found only once, and based on their low frequency they may be either mutations or true alleles. The first variant, candidate allele K18.1', had an envelope sequence identical to K18.1 but a divergent 3′ LTR. The second variant, candidate allele K18.2/3′, had an envelope sequence intermediate between K18.2 and K18.3 (Y at position 97; W at position 154; V in positions 272 and 348; I at position 534; [Figure 1B]).

The unambiguous assignment of IDDMK$_{1,2}$22 to HERV-K18 had not been made previously for two reasons: first, because only HERV-K18 LTR sequences had been available, and second, the published HERV-K18 LTR sequence turned out to be identical to K18.2, which is

as distantly related to the IDDMK$_{1,2}$22/K18.1 and K18.3 LTRs as it is from the HERV-K10 LTRs (∼7%). This explains why the IDDMK$_{1,2}$22/K18.1 LTR sequence originally appeared as an independent entity, identical neither to K18 nor to K10. Finally, an extended locus on chromosome 1 also comprising CD48/HERV-K18 is a candidate susceptibility region for type I diabetes (Mein et al., 1998).

Expression of HERV-K18 in the CD48 Locus but Not of Other Known HERV-K Proviruses Is Induced by IFN-α$_{1/2}$ with Rapid Kinetics in PBL of All K18 Genotypes and Is Restricted to Non-T Cells

We next sought to establish how exogenous viruses could induce SAg expression. Type I IFNs are key regulators of the innate host response to viruses. Therefore, we asked whether SAg expression was regulated via IFN-α. An initial hurdle was to discriminate unambiguously HERV-K18 RNA from RNA of closely related, human-specific HERV-K proviruses. The latter can be separated in two groups within the SAg coding region, one represented by HERV-K108 and the other by HERV-K104. As shown in Figure 2A, transcripts from both groups can be distinguished from HERV-K18 RNA by ribonuclease protection with a probe positioned in the SAg coding region. This permits study of HERV-K18 expression in response to stimuli such as type I and II IFNs and lipopolysaccharide (LPS). In fact, as shown in Figure 2B, HERV-K18 expression was inducible by IFN-α$_{1/2}$ with rapid kinetics in PBL of healthy individuals. The known HERV-K proviruses were not inducible by IFN-α$_{1/2}$ and were constitutively expressed in PBL. The mean induction of HERV-K18 in PBL was ∼5-fold in 23 genetically different individuals (5 ± 3.2), as determined by quantitative comparison with the TATA binding protein (TBP). This is an underestimation by a factor of approximately 3, because the SAg is induced only in
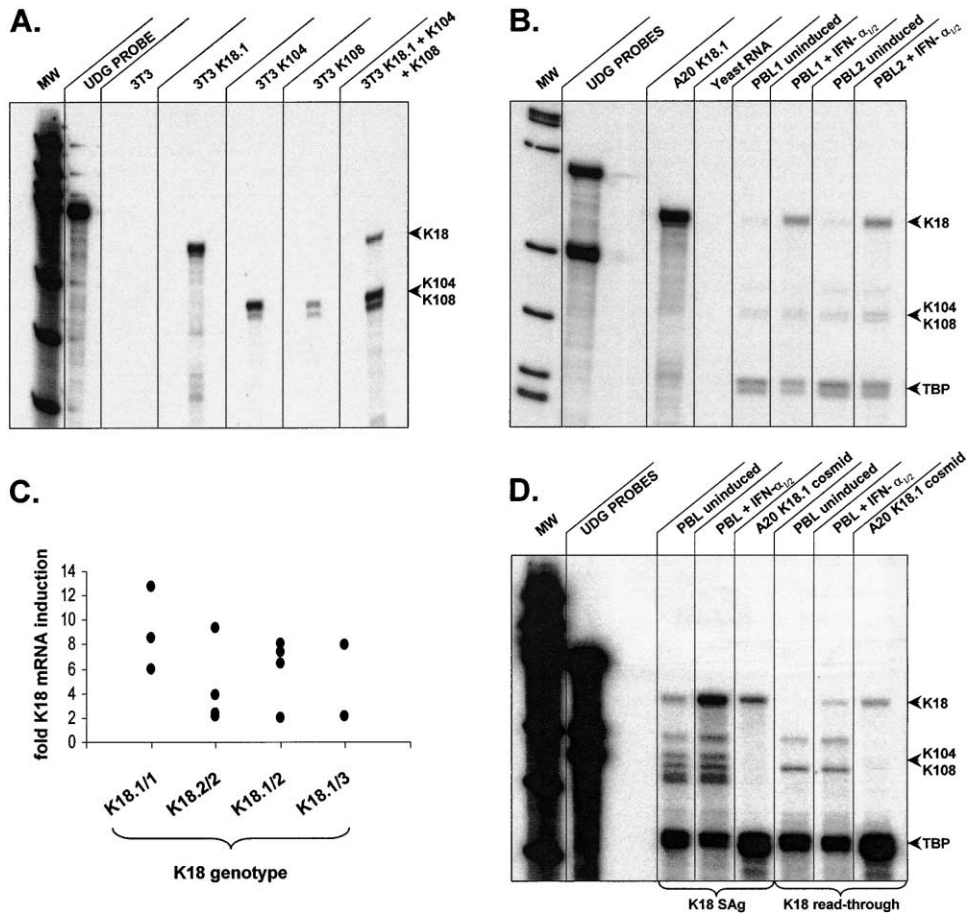
Figure 2. Expression of HERV-K18 but Not of Other Known HERV-K Proviruses Is Induced by IFN-$\alpha_{1/2}$ with Rapid Kinetics in Primary Leukocytes of All K18 Genotypes

(A) A riboprobe positioned in the HERV-K18 SAg coding region discriminates the SAg from other known HERV-K envelope transcripts. RNA from the following conditions was hybridized with the K18 probe: the HERV-free mouse fibroblast cell line 3T3; 3T3 transfected with the envelope allele K18.1; 3T3 transfected with the K104 envelope gene; 3T3 transfected with the K108 envelope gene; and an equimolar mix of the above. The arrowhead on the top indicates the fragment protecting the K18 transcript and the arrowhead at the bottom indicates the fragment protecting the K104 and K108 transcripts.

(B) HERV-K18 expression is strongly induced by IFN-$\alpha_{1/2}$ with rapid kinetics. PBL from two healthy individuals were induced with IFN-$\alpha_{1/2}$ for 1 hr. RNA from A20 mouse cells transfected with constructs expressing the HERV-K18 envelope, yeast RNA, and RNA from uninduced and induced PBL samples were hybridized with the K18 probe. Arrowheads indicate the protected fragments specific for K18, K104/108, and human TBP as internal control.
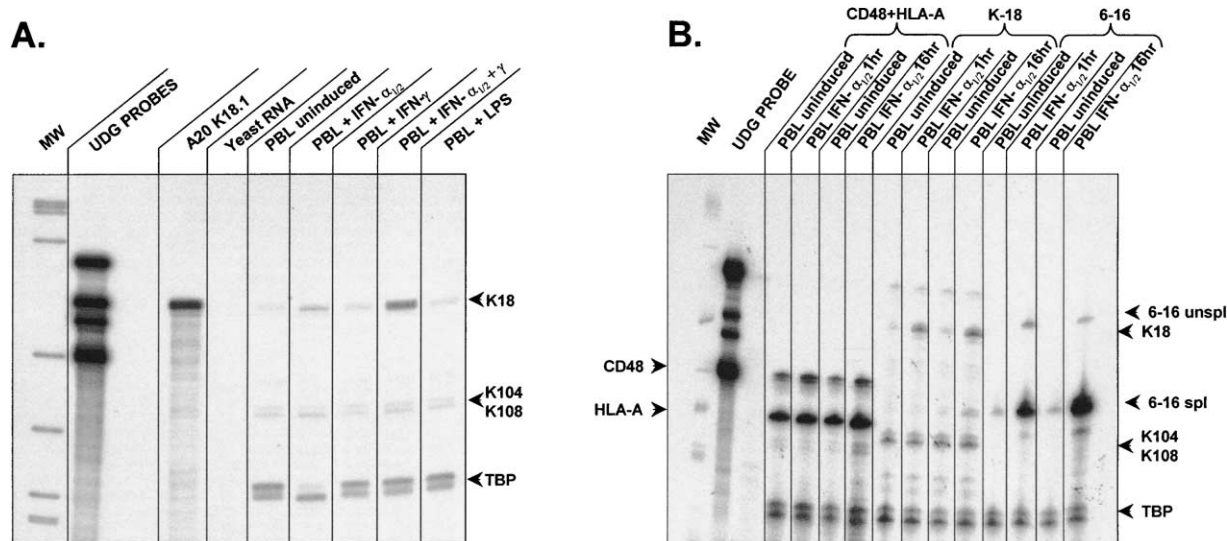
(C) HERV-K18 expression is strongly induced by IFN-$\alpha_{1/2}$ in all K18 genotypes. The mean K18 mRNA induction in 23 PBL samples from healthy donors was 5 ± 3.2, as quantified by Phospho-Imager and corrected for the uninduced control TATA binding protein (TBP). Strong transcriptional K18 inductions were obtained for all K18 genotypes.

(D) HERV-K18 expression induced by IFN-α is derived from the CD48 locus. RNA from uninduced and IFN-$\alpha_{1/2}$-induced PBL, from mouse A20 cells transfected with a cosmid bearing the complete K18 provirus, were hybridized with the K18 SAg probe and with a probe comprising both the 3′ proviral LTR and the flanking CD48 intron ("read-through" probe). The read-through probe detects only unspliced transcripts from the CD48 locus. Arrowheads indicate the fragments specific for K18 SAg transcripts on the left-hand panel and K18 read-through transcript on the right panel.

CD2⁻ non-T cells, which constitute less than 30% of PBL (see supplemental data S1 at http://www.immunity.com/cgi/content/full/15/4/591/DC1). With this in mind, strong inductions were found for all K18 genotypes (Figure 2C). A riboprobe that discriminated expression of individual K18 alleles confirmed that all alleles were similarly induced by IFN-$\alpha_{1/2}$ (S.M., unpublished data).

Identical HERV-K18 transcripts could still derive from multiple loci. The vast majority of nascent transcripts is not cleaved at the polyadenylation site and contains heterogeneous 3′ termini (Wuarin and Schibler, 1994).

We therefore generated a riboprobe that specifically detects HERV-K18 read-through transcripts, which were elongated into the CD48 intron and were not yet cleaved. The extent of induction of these read-through transcripts was comparable to that of the HERV-K18 SAg, namely ∼5-fold and ∼7-fold, respectively (Figure 2D). This suggests that the IFN-α-induced SAg RNA was derived from the CD48 locus and is also consistent with transcriptional activation of HERV-K18 by IFN-α. In essence, within the family of constitutively expressed HERV-K proviruses, HERV-K18 in the CD48 locus was excep-

A.

MW | UDG PROBES | A20 K18.1 | Yeast RNA | PBL uninduced | PBL + IFN-$\alpha_{1/2}$ | PBL + IFN-γ | PBL + IFN-$\alpha_{1/2}$ + γ | PBL + LPS

◄ K18
◄ K104
◄ K108
◄ TBP

B.

CD48+HLA-A | K-18 | 6-16

MW | UDG PROBE | PBL uninduced | PBL IFN-$\alpha_{1/2}$ 1hr | PBL uninduced | PBL IFN-$\alpha_{1/2}$ 16hr | PBL uninduced | PBL IFN-$\alpha_{1/2}$ 1hr | PBL uninduced | PBL IFN-$\alpha_{1/2}$ 16hr | PBL uninduced | PBL IFN-$\alpha_{1/2}$ 1hr | PBL uninduced | PBL IFN-$\alpha_{1/2}$ 16hr

CD48 ►
HLA-A ►

◄ 6-16 unspl
◄ K18
◄ 6-16 spl
◄ K104
◄ K108
◄ TBP

Figure 3. IFN-$\alpha_{1/2}$-Regulated HERV-K18 Expression Is Canonical and Distinct from CD48

(A) The strong HERV-K18 induction with rapid kinetics is specific for IFN-α and is superinduced by IFN-γ. An experiment similar to Figure 2B was performed. The following experimental conditions were included in addition: PBL induced with IFN-γ alone, PBL induced with IFN-$\alpha_{1/2}$ + γ, and PBL induced with LPS.

(B) The classical IFN-α target gene 6-16 is induced similarly to the SAg in primary PBL while CD48 and the MHC class I isotype HLA-A are induced weakly by IFN-$\alpha_{1/2}$ with slow kinetics. PBL from a healthy blood donor were induced with IFN-$\alpha_{1/2}$ for 1 and 16 hr or cultured for the same time without treatment. Total RNA was hybridized with probes specific for CD48, HLA-A, K18 SAg, 6-16, and TBP as control. The 6-16 probe was designed to contain both the last exon and adjacent 3′ intron. Both unspliced (6-16 uspl) and spliced transcripts (6-16 spl) were detected.

tional regarding its low uninduced expression levels and its IFN-α inducibility restricted to non-T cells of all HERV-K18 genotypes.

IFN-$\alpha_{1/2}$-Regulated HERV-K18 Expression Is Canonical and Distinct from CD48

We first asked whether HERV-K18 behaves as a classical IFN-α target gene or whether stimuli such as type II IFNs and LPS also induce K18 expression. IFN-γ and LPS alone had no stimulatory effect but combined treatment of PBL with IFN-$\alpha_{1/2}$ + IFN-γ superinduced HERV-K18 expression (Figure 3A). Thus, while type II IFNs and LPS per se were not sufficient to induce HERV-K18 expression, IFN-γ synergistically augmented IFN-α induction, an effect known as IFN-γ priming (Levy et al., 1990). NF-κB inducing agents such as LPS and PMA alone (Sutkowski et al., 2001) were not sufficient to induce HERV-K18 expression.

We next compared the kinetics and magnitude of SAg induction in PBL with that of a classical IFN-α target gene 6-16 (Ackrill et al., 1991), the MHC class I isotype HLA-A, and CD48. CD48 has been proposed to be inducible by both type I and type II IFNs in certain cell lines (Tissot et al., 1997). Two differences were apparent: first, uninduced CD48 expression was higher than uninduced SAg expression, which was low in the absence of induction; second, CD48 was induced less rapidly and less strongly than the SAg, namely less than 2-fold after 1 and 16 hr instead of ~5-fold after 1 hr of IFN-$\alpha_{1/2}$ exposure (Figure 3B). This was particularly true for primary leukocytes, where CD48 was not IFN-$\alpha_{1/2}$ inducible at all in certain donors. In that respect, CD48 was comparable to HLA-A, an MHC class I isotype known to be only

weakly IFN-α inducible (Hakem et al., 1991) (Figure 3B). In contrast, the classical IFN-α target gene 6-16 was as strongly and rapidly induced in PBL as the SAg, namely ~15-fold after 1 hr of treatment (Figure 3B). Spliced and unspliced 6-16 transcripts were both induced. The transient accumulation of unspliced, nascent 6-16 transcripts is consistent with transcriptional activation of the 6-16 gene by IFN-$\alpha_{1/2}$. Finally, while IFN-α-induced HERV-K18 expression was specifically restricted to CD2$^-$ non-T cells (see supplemental data S1 at http://www.immunity.com/cgi/content/full/15/4/591/DC1), expression of 6-16 was equally inducible in both T and non-T cells, and the weak HLA-A and CD48 inductions appeared to be more pronounced in T cells (see supplemental data S2 at http://www.immunity.com/cgi/content/full/15/4/591/DC1). These experiments indicate that IFN-$\alpha_{1/2}$-regulated HERV-K18 expression is distinct from CD48, regarding the cellular subset in which it is induced, the magnitude and kinetics of induction, as well as the signaling pathways used. Thus, HERV-K18 expression in the CD48 locus, but not expression of known HERV-Ks in other chromosomal locations, was strongly induced with rapid kinetics by IFN-$\alpha_{1/2}$ but not IFN-γ and was superinduced by IFN-γ priming. In essence, HERV-K18 behaves as a canonical IFN-α target gene with respect to all stimuli analyzed.

IFN-$\alpha_{1/2}$-Induced HERV-K18 Expression Produces a T Cell Mitogenic Effect in All K18 Genotypes

We then reasoned that induction of HERV-K18 expression was expected to result in SAg function. In fact, PBL induced with IFN-$\alpha_{1/2}$ exerted a mitogenic effect on syngeneic T cells and efficiently induced T cell blast
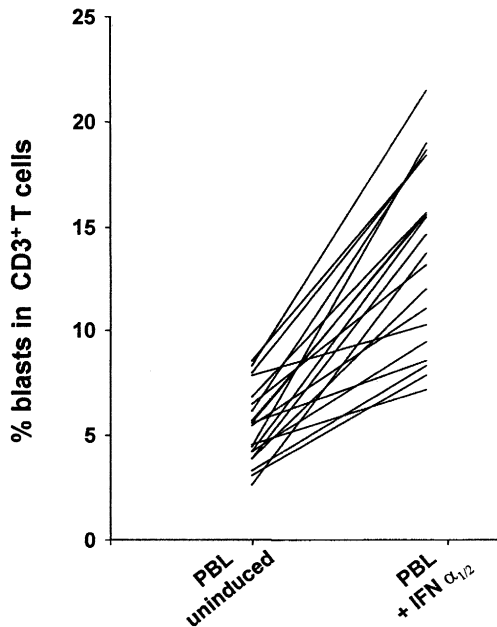
Figure 4. IFN-α$_{1/2}$-Induced HERV-K18 Expression Produces a T Cell Mitogenic Effect in All K18 Genotypes

(A) PBL from 21 healthy blood donors were cultured for 1 hr in the presence or absence of IFN-α$_{1/2}$, washed, and added back to syngeneic PBL at equal ratios. After 2 ½ days of culture, IL-2 was added for the last 24 hr. The percentage of blasts within the CD3$^+$ T cell population was determined by FACS, in uninduced and IFN-α-treated samples. As shown supplemental data S5 (see http://www.immunity.com/cgi/content/full/15/4/591/DC1), strong inductions of T cell blasts were found in all K18 genotypes.

formation in all individuals analyzed (Figure 4; supplemental data S5 at http://www.immunity.com/cgi/content/full/15/4/591/DC1). An exception to this rule was only three individuals with high uninduced levels of >15% blasts in CD3$^+$ T cells. Strong inductions of T cell blasts were found in all K18 genotypes, suggesting that all allelic K18 combinations were similarly mitogenic (supplemental data S5 at http://www.immunity.com/cgi/content/full/15/4/591/DC1). Polymorphic genetic factors other than the HERV-K18 genotype may influence blast formation and could account for some of the differences observed. For instance, different MHC class II isotypes and alleles differ in their capacity to bind and present both bacterial and endogenous SAgs of mice (Herman et al., 1990; Subramanyam et al., 1993). Whether this also applies for human endogenous SAgs will be addressed elsewhere. In essence, all HERV-K18 genotypes were induced similarly by IFN-α$_{1/2}$ and exerted a comparable mitogenic effect.

IFN-α-Induced HERV-K18 Expression Specifically Activates Sag-Reactive CD4$^+$ Vβ7 T Cells

We next analyzed whether IFN-α induction of APCs specifically activates Sag-reactive Vβ7 T cells. To answer this question we used two independent assays, one that analyzes expression of the early T cell activation marker CD69 (Simms and Ellis, 1996) on Sag-reactive and control T cells, and the other that measures Vβ-specific accumulation of T cell blasts (Kappler et al., 1989). IFN-

α$_{1/2}$-treated PBL were used as APCs and cultured at different ratios with T cells. After 24 hr, CD69 expression was analyzed on total T cells, Sag-reactive Vβ7 T cells, and control Vβ families. The unrelated Vβ2 and Vβ12 T cells were selected because anti-Vβ12 and -Vβ7 antibodies (Ab) share the same isotype, and Vβ2 T cells represent the single largest subset in the repertoire. In two individuals homozygous for K18.1, IFN-α-induced APCs activated 10%–30% of syngeneic T cells in a dose-dependent fashion (Figure 5A). The levels of IFN-α-induced transcriptional K18 activation correlated with the strength of T cell activation. Namely, donor 1 with 12.7-fold transcriptional K18 induction had stronger T cell activation than donor 2, which had an 8.5-fold K18 induction (supplemental data S5 at http://www.immunity.com/cgi/content/full/15/4/591/DC1). When CD69 expression was analyzed on the Vβ subsets of these two donors, Vβ7 T cells were stimulated more efficiently than control Vβs (Figures 5B and 5C). This was also true for an individual homozygous for K18.2 (Figure 5D). While CD4$^+$ and CD8$^+$ T cells were equally found among T cell blasts before and after culture with untreated and IFN-α-induced APCs, Vβ7 T cells carrying the CD4$^+$ but not the CD8$^+$ coreceptor appeared to be selectively activated by IFN-α-induced APCs, consistent with notion that HERV-K18 SAgs preferentially activate CD4 T cells (see supplemental data S3 at http://www.immunity.com/cgi/content/full/15/4/591/DC1). This is supported by the fact that SAg- reactive T cell hybrids are absolutely CD4 dependent (Sutkowski et al., 2001; our unpublished data).

Furthermore, Vβ7 and to a lesser extent Vβ13 T cells accumulated preferentially among T cell blasts in response to IFN-α-treated PBL of five different individuals, as compared to Vβ12 (see supplemental data S6 at http://www.immunity.com/cgi/content/full/15/4/591/DC1). In support of this, Vβ7$^+$ T cells were also specifically enriched among T cells cultured with A20 transfectants expressing K18.1, but not a K18.1 mutant with a premature frameshift mutation (F.M., submitted). In these experiments, Vβ7 enrichments correlated with the presence of T cell proliferation. These finding are consistent with the fact that Vβ7 is a high-affinity Vβ chain for the endogenous K18 SAgs and are also consistent with a quantitative model of T cell activation by the SAg. According to this model, T cells carrying high-affinity Vβ chains are stimulated by the lowest doses of SAg and at the highest SAg doses all T cells are eventually stimulated (Fleischer et al., 1991). In essence, IFN-α treatment of PBL induced a T cell mitogenic activity consistent with specificity for SAg-reactive Vβ7$^+$ CD4 T cells in all K18 genotypes analyzed.

IFN-α-Induced Expression of the Endogenous HERV-K18 Locus Activates SAg-Reactive T Cells Similarly to the Transfected HERV-K18 Alleles

We next confirmed that the IFN-α-induced endogenous K18 locus induces T cell proliferation similarly to transfected K18 alleles. In fact, the capacity of IFN-α-treated PBL from a K18.1/3 heterozygous individual to stimulate proliferation of purified, syngeneic Vβ7 T cells was comparable to that of the transfected K18.1 and K18.3 alleles (Figure 6A). Compatible with IFN-α-mediated transcrip-
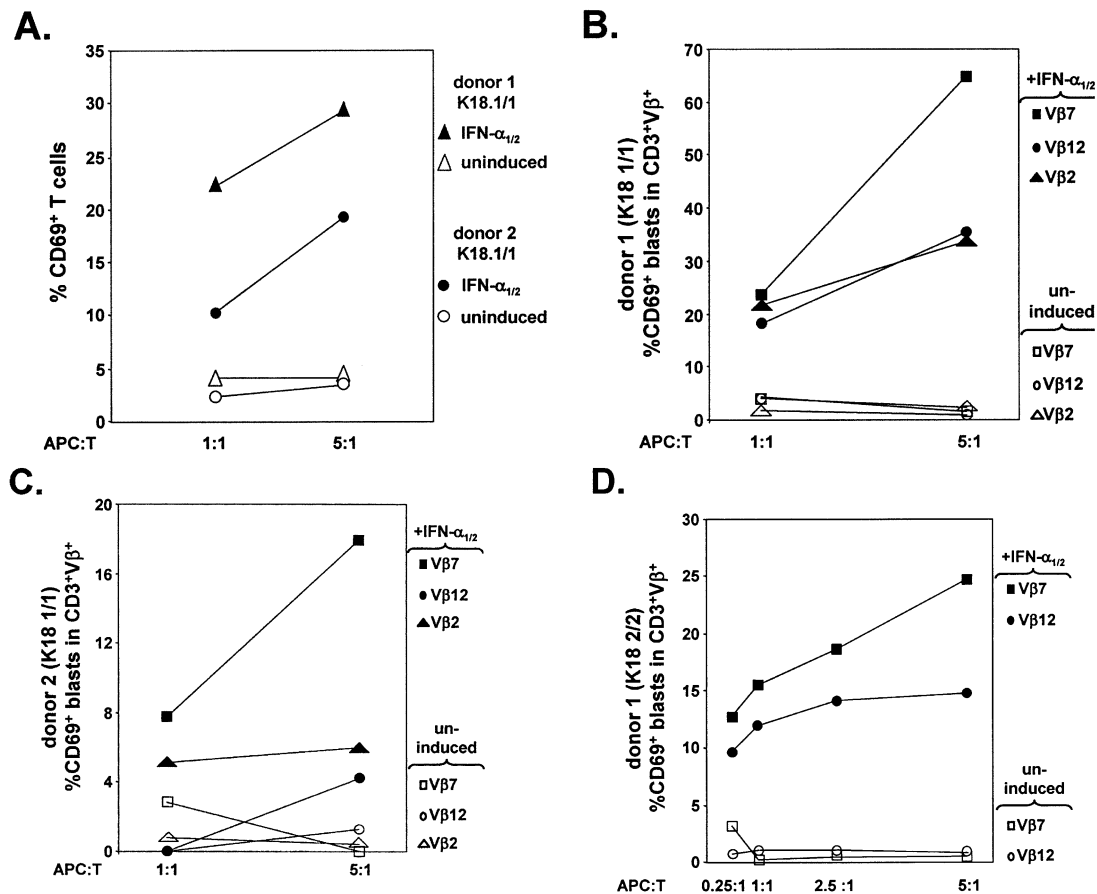
A.

B.

C.

D.

Figure 5. IFN-α-Induced HERV-K18 Expression Specifically Activates SAg-Reactive CD4$^+$ Vβ7 T Cells

(A) IFN-$\alpha_{1/2}$-treated PBL (APCs) activate syngeneic T cells dependent on the dose of APC and the strength of transcriptional K18 induction. PBL from two individuals homozygous for K18.1 were induced with IFN-$\alpha_{1/2}$. Donor 1 had a transcriptional induction of 12.7 and donor 2 had 8.5. IFN-$\alpha_{1/2}$-treated and untreated APCs were cultured with syngeneic T cells at the indicated ratios for 24 hr and expression of the early T cell activation marker CD69 was analyzed.

(B–D) IFN-$\alpha_{1/2}$ activates SAg-reactive Vβ7 T cells preferentially, as revealed by expression of the early T cell activation marker CD69 and preferential accumulation of Vβ7, and to a lesser extent Vβ13 in T cell blasts. Expression of CD69 was analyzed on CD3$^+$Vβ$^+$ T cells after culture for 24 hr with different doses of unstimulated and IFN-$\alpha_{1/2}$-induced PBL (APCs) of donors 1 (B) and 2 (C) shown in 5A, as well as APCs from a donor homozygous for K18.2 (D). Shown are the results obtained with CD69$^+$ blasts. In supplemental data S6 (see http://www.immunity.com/cgi/content/full/15/4/591/DC1), the specific accumulation of Vβ7 and Vβ13 in blasting T cells after 3 ½ days of culture with IFN-$\alpha_{1/2}$-treated syngeneic APCs was analyzed. Donor 2 had exceptionally high uninduced levels of Vβ12$^+$ blasts that were not further increased with SEB treatment, and donor 5 had exceptionally high uninduced levels of Vβ7$^+$ blasts that were not further increased with IFN-α treatment.

tional activation of K18 in APCs, purified B lymphocytes induced with IFN-α_{2a} stimulated proliferation of syngenic T cells with rapid kinetics, comparably to the polyclonal mitogen PHA (Figure 6B). Collectively, IFN-α treatment of PBL and purified APCs induced the endogenous SAgs similarly to the SAg function encoded by transfected K18 envelope alleles.

Antibodies that Bind the SAg in Solution Inhibit SAg Function of the IFN-α-Induced HERV-K18 Locus Similarly to that of the Transfected HERV-K18 Alleles
To firmly establish that IFN-α-induced SAgs are encoded by HERV-K18, an attempt was made to specifically inhibit the SAg with anti-HERV-K18 envelope antibodies. Two independent batches of antisera against N- and C-terminal SAg peptides were obtained by immunizing rabbits on separate occasions. The peptide anti-

sera but not the respective preimmune serum were capable of immunoprecipitating the SAg-HA fusion protein as efficiently as anti-HA Abs (Figure 7A). Therefore, the antisera contained Abs that were able to bind the SAg in solution. Next, crude antisera and affinity-purified fractions from two independent immunizations were compared with preimmune sera and with flow-through fractions depleted of peptide-reactive Abs for their capacity to inhibit SAg function. In fact, the peak fraction of affinity-purified IgGs from the first batch raised against the N-terminal peptide (α-N P-IgG1) inhibited the generation of blasts as consistently and efficiently as monoclonal anti-MHC class II Abs directed against HLA-DR, L243 (Figure 7B). Importantly, no significant blast inhibitions were obtained for control Abs, such as polyclonal Abs raised against recombinant HERV-K envelope protein (85% and 63% of rabbit serum values)
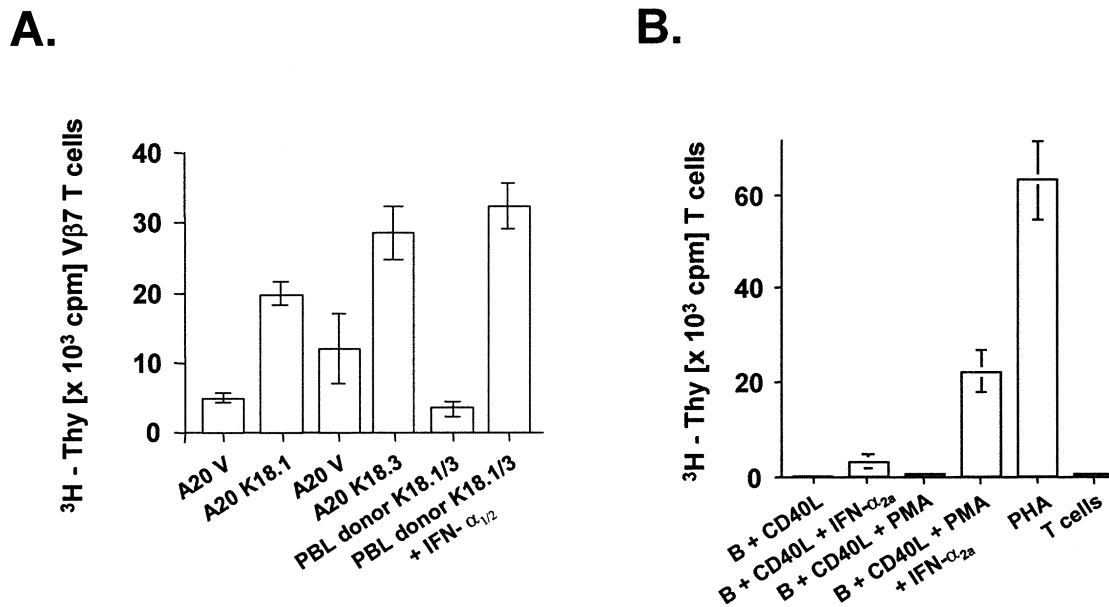
A.

B.

Figure 6. IFN-α-Induced Expression of the Endogenous HERV-K18 Locus Activates SAg-Reactive T Cells Similarly to the Transfected HERV-K18 Alleles

(A) SAg-reactive Vβ7[+] human T cells were stimulated similarly by stably SAg transfected mouse B lymphoma cells (A20) and by IFN-α-induced syngeneic APCs. Transfectants expressing the following constructs were used: the truncated envelope allele K18.1, the full-length envelope K18.3, and the respective vector controls. As primary APCs, untreated PBL and IFN-$\alpha_{1/2}$-induced PBL from a donor heterozygous for K18.1/3 were used. After 48 hr of culture, ^{3}H-Thymidine incorporation of purified primary Vβ7 T cells was measured.

(B) Purified B cells cultured in the presence of CD40L were induced with IFN-α_{2a}, treated with PMA, and used to stimulate syngeneic T cells. After 48 hr of culture, ^{3}H-Thymidine incorporation was measured.

and the respective preimmune serum (78% and 64% of rabbit serum values). In addition, the peak fraction of affinity-purified IgGs raised against the C-terminal SAg peptide only marginally inhibited blasts, if at all (Figure 7B). Thus, while both the anti-N and -C antisera were able to bind the SAg in solution, only anti-N Abs inhibited SAg function as efficiently as anti-HLA-DR Abs.

Likewise, the crude anti-N antiserum obtained from the second immunization (α-N S2) but not the respective preimmune serum inhibited activation of SAg-reactive Vβ7 T cells by transfectants constitutively expressing the K18.3 SAg (Figure 7C). This inhibition was, first, efficient, because it inhibited Vβ7 T cell proliferation to levels observed with vector transfected APCs and, second, specific, because PHA-induced polyclonal activation was not influenced.

To confirm the specificity of this inhibition, we compared the peak fraction of affinity-purified IgGs and the flow-through fraction depleted of peptide-reactive Abs from the second immunization for their ability to inhibit IFN-α-induced T cell blast formation. As determined by ELISA, peptide reactivity was significantly enriched and carrier reactivity was significantly diminished in affinity-purified as compared to flow-through fractions. As shown in Figure 7D, the capacity to inhibit SAg function had been depleted from the flow-through fraction, yet it was present in the affinity-purified IgGs (see also supplemental data S4 at http://www.immunity.com/cgi/content/full/15/4591/DC1). Shown is the average of two independent experiments with IFN-α-induced T cell blasts from a single donor. The generation of IFN-α-induced blasts was inhibited in a dose-dependent fash-

ion by affinity-purified α-N IgGs, and this inhibition was lost upon depletion of α-N Abs. Inhibition of IFN-α-induced blast formation with crude α-N antisera was less consistent than it was in assays with the transfected SAg (Figure 7C). In Figure 7E, the observation is extended to four additional, independent donors. While there was a significant inhibition of IFN-α-induced T cell blast formation with affinity-purified α-N IgGs in all donors (p = 0.02, t-Test), the immunodepleted fraction had lost this ability (p = 0.01, t-Test). The affinity-purified Abs from the second immunization (Figure 7E) appeared to inhibit less efficiently than the corresponding fraction from the first batch (Figure 7B). However, this could also be explained by the overall less stronger induction of T cell blasts in Figure 7E. In summary, two independent batches of anti-peptide antisera and affinity-purified IgG fractions bound the SAg in solution and inhibited the SAg function of the IFN-α-induced endogenous K18 locus and of the transected K18 gene. This inhibition was removed by immunodepletion of peptide-reactive Abs. These experiments therefore suggest that the IFN-α-induced blast formation is generated by the HERV-K18 SAgs and not by other IFN-α-induced target genes.

During attempts to titrate different type I IFN preparations, we noticed a differential responsiveness of the K18 locus to IFNs. The chimeric IFN-$\alpha_{1/2}$ induced K18 at least 3 times more strongly than IFN-α_{2a} and IFN-β (S.M., unpublished data). This appeared to be specific for K18, because the control gene 6-16 was induced with equal efficiency by these different IFN isotypes. It prompted us to analyze whether this differential transcriptional responsiveness of K18 would be reflected in a differen-
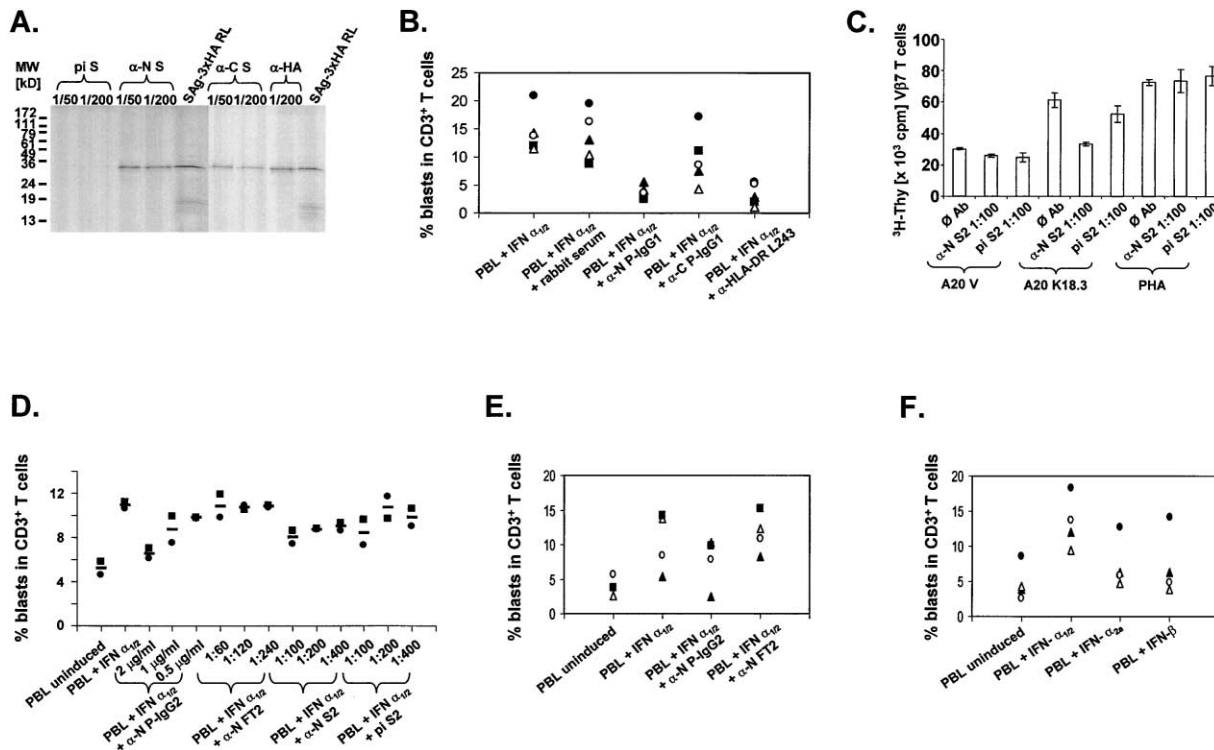
Figure 7. The Function of IFN-$\alpha_{1/2}$-Induced SAgs Is Inhibited by Anti-HERV-K18 Antibodies and Correlates with the Strength of Transcriptional K18 Activation

(A) Polyclonal anti-K18 peptide Abs bind the SAg protein in solution. Rabbit antisera were raised against N- and C-terminal K18.1 peptides. A C-terminal 3xHA SAg fusion protein was produced in reticulocyte lysates (SAg-3HA RL). Anti-N (α-N S) and -C antisera (α-C S), but not the respective preimmune serum (pi S), were capable of immuno-precipitating the SAg fusion as efficiently as anti-HA antibodies (α-HA).

(B) Normal rabbit serum, the peak fractions from the first batch of affinity-purified IgGs raised against N- and C-terminal K18.1 peptides (α-N P-IgG1; α-C P-IgG1), and the anti-HLA-DR monoclonal antibody L243, were added to PBL cultures from five healthy individuals, which had been induced by IFN-$\alpha_{1/2}$. The assay was performed as in Figure 4; the percentage of T cell blasts obtained in the presence of normal rabbit serum is shown as a reference.

(C) Stimulation of SAg-reactive Vβ7$^+$ T cells by K18.3 transfectants is inhibited by the second batch of crude anti-N antiserum (α-N S2). Vβ7 T cells were stimulated by mouse A20 cells transfected with the full-length envelope allele K18.3 or with the vector control. After 48 hr of culture, ^{3}H-Thymidine incorporation was measured. Cells were cultured in the presence of anti-N (α-N S2) or the respective preimmune serum (pi S2).

(D) Depletion of anti-N Abs removes the inhibition of SAg function. The peak fraction from the second batch of affinity-purified IgGs (α-N P-IgG2) and the flow-through fraction (α-N FT2) depleted of α-N-reactive Abs were compared with the crude antiserum (α-N S2) and preimmune serum (pi S2) for their ability to inhibit IFN-$\alpha_{1/2}$-induced T cell blast formation. The average of two independent experiments with IFN-α-induced T cell blasts from a single donor is shown. The crude α-N antiserum was less consistently inhibiting blast formation than the function of the transfected K18 SAgs (C).

(E) Depletion of anti-N Abs removes the inhibition of SAg function. The peak fraction from the second batch of affinity-purified IgGs (α-N P-IgG2) and the corresponding flow-through fraction (α-N FT2) were compared for their ability to inhibit IFN-$\alpha_{1/2}$-induced T cell blast formation of four donors.

(F) K18 is induced differentially by type IFNs and this correlates with the strength of the SAg response. IFN-$\alpha_{1/2}$ induces K18 transcription ~3 times stronger than IFN-α_{2a} and IFN-β. PBL from four donors were treated with IFN-$\alpha_{1/2}$, IFN-α_{2a} and IFN-β for 1 hr and then cultured with syngeneic PBL. The percentage of blasts in the T cell population was determined as before.

tial blastogenesis, and that is precisely what was found—the IFN-$\alpha_{1/2}$ that most efficiently induced K18 transcriptionally also generated most potently T cell blasts (Figure 7F). Given that different IFN isotypes and preparations induce other type I IFN target genes with similar efficiency (Der et al., 1998), this is an additional argument to suggest that the generation of blasts is the result of K18 induction. Therefore, these experiments strongly suggest that the IFN-α-induced endogenous HERV-K18 locus encodes MHC class II-dependent SAgs in all K18 genotypes, comparable to the SAgs encoded by the transfected HERV-K18 envelope genes.

These observations could have at least two important consequences. First, endogenous HERV-K18 SAgs induced by viral infections via IFN-α provide a model linking environmental factors and disease. Diverse viruses may trigger autoreactive T cells via induction of endogenous SAgs, but autoimmunity will develop only in individuals that carry some or all genes conferring susceptibility to disease. Second, SAg-induced immune stimulation was proposed to amplify mouse mammary tumor virus infection and to favor viral transmission (Held et al., 1993). By analogy, endogenous HERV-K18 SAgs may amplify immune responses during acute and chronic infections by exogenous viruses. This may favor the establishment of viral persistence and latency in the

course of acute infections and may be a cofactor during reactivation of persistent infections (Sutkowski et al., 2001).

While IFN-α-induced endogenous K18 SAgs constitute a novel mechanism that could cause autoimmunity, many previously known IFN-α target genes may act independently of, or jointly with, the SAg. Indeed, type I IFNs exert pleiotropic actions on the innate and adaptive immune system; for example, they activate and mature macrophages and dendritic cells, induce isotype switching of B cells, and keep activated T cells alive (Le Page et al., 2000). It is also clear that the previously reported preliminary association of extracellular IDDMK$_{1,2}$22 transcripts with disease requires revision. First, none of the K18 alleles has functional *gag* or *pol* genes that could be responsible for RT activity or particle production and accordingly for the specific extracellular accumulation of K18 transcripts. Therefore, the presence of extracellular K18 transcripts does not reflect biological activity of the K18 provirus and SAg function. Second, the newly described K18 polymorphism demonstrates that the genetic diversity between alleles of the same K18 provirus can be as great as the variability between individual HERV-K proviruses on different chromosomes. This unpredicted feature redefines the molecular K18 species and, as a consequence, also its detection. In summary, these observations invalidate the earlier described preliminary association of extracellular IDDMK$_{1,2}$22 transcripts with disease. However, we provide independent and novel evidence that indicate how K18 SAgs may be associated with the onset of type I diabetes, namely via IFN-α-regulated expression. Increased levels of circulating IFN-α and viral infections have been tightly linked with the onset of type I diabetes. In essence, IFN-α-induced SAgs may link environmental factors and particularly viral infections with the onset of autoimmunity.

A specific accumulation of Vβ7 T cells had been described in the pancreas and to a lesser extent in the spleen of patients dying at the onset of type I diabetes from a rare metabolic complication (Conrad et al., 1994). Given the rarity of the event, only a few studies exist. The technically most comparable study analyzed the infiltrating T cell repertoire molecularly (Somoza et al., 1994) and resulted in findings consistent with ours, namely that Vβ7 is the single most dominantly used TCR in the pancreas at disease onset. In the second study (Hanninen et al., 1992), only four Vβ families excluding Vβ7 were analyzed by immuno-fluorescence and therefore direct comparisons cannot be made. However, a recent study analyzed the TCR usage in the circulation of patients before, at, and after disease onset and compared it with that of age-, sex-, and HLA-matched controls (Luppi et al., 2000). In this study, circulating levels of Vβ7 and to a lesser extent of Vβ13 T cells were higher before and at disease onset, and higher in diabetics than in healthy controls. These results are consistent with a model in which viral infections induce K18 SAg expression in circulating APCs, which causes activation and proliferation of circulating Vβ7 and Vβ13 T cells in type I diabetes. Finally, persistence of viral infections in pancreatic β cells and/or a chronic local IFN-α response could be cofactors in causing Sag-dependent disease. Inhibition of SAg function in vivo during different stages

of the clinical disease will be required to dissect the precise role of the SAg in causing pathology.

Experimental Procedures

Genetic Characterization of HERV-K18

To position the K18 envelope gene and 5′ LTR with respect to the first and second CD48 exon, PCR was performed with primers CD48E1F and K18BIF and CD48I1F and CD48E2R, respectively. The *env*-LTR fragments of K18 proviruses from 60 different individuals were amplified by PCR with primers K18UTR and K18FLR. PCR products were directly sequenced and subcloned and the presence of all polymorphic sites was confirmed on single molecular clones by sequencing (GenBank accession number AF012336).

K18 typing by PCR and restriction analysis. A 1096 bp fragment containing the 3′ K18 LTR was amplified with primers K18LTR3 and K18FLR. The product was digested with BstNI and NsiI and analyzed on 8% PAGE, which allowed discriminating of all K18 genotypes.

Oligonucleotides. 1. Mapping of K18 provirus in CD48 gene.
CD48E1F 5′-CACAGATCTAGAACTAGTGCCACCATGTGCTCCA GAGGTTGG-3′;
K18BIF 5′-CTGTCATTTGGATGGGAGACAGGC-3′;
CD48I1F 5′-CACGGATCCCAGATTCCGCTTATGTTGTACATGC-3′;
CD48E2R 5′-CACGTCGACGGAGACCACGGTCATATGTACCAAGT GAC-3′.

2. Amplification of K18 *env* gene.
K18UTR 5′-ATCAGAGATGCAAAGAAAAGC-3′;
K18FLR 5′-ATTGCGGCCGCTCAGTCGACCCCAAACCTTTAAAT ATTGTCTCATG-3′;
K18Kzk 5′-ATCAGATCTAACACTAGTGCCACCATGGTAACACCA GTCA-3′;
K18/1689 5′-ATTGCGGCCGCTCATGCGACTTACTTATTCATTCA TGGCCC-3′.

3. Sequencing of K18 *env* gene.
Amino acid position (aa) 97, 5′-ATCAGATCTAACACTAGTGCCA CCATGGTAACACCAGTCACATGG-3′; aa 154 and 272, 5′-AGAATG TGTGGCCAATAGTGT-3′; aa 272, 5′-ATGGATGGCGAGGCCTCC CAC-3′; aa 348, 5′-AGAGAAGGCATGTGGATCCCT-3′.

4. Amplification of K108 env gene.
K108UTR 5′-ATCAGATCTAACACTAGTCGCTTCACCAGGAGAAA ATCAGC-3′; K108FLR 5′-ATTGCGGCCGCTCAGTCGACATTGTCG GGAGTTCAAGACCAGC-3′; K108Kzk 5′-ATCAGATCTAACACTAGT GCCACCATGGACCCATCAGAGATGC-3′; K108/1689 5′-ATTGCG GCCGCTCAGTCGACTTACTTATTCATCTACACAGACACAGTAACA ATC-3′.

5. Amplification of K104 *env* gene.
K104UTR 5′-ATCAGATCTAACACTAGTCGCTTCACCAGGAGAAA ATCAGC-3′; K104FLR 5′-ATTGCGGCCGCTCAGTCGACATTGTCT ATTGAGATAATCATGAGG-3′; K104Kzk 5′-ATCAGATCTAACACTA GTGCCACCATGGACCCATCGGAGATGC-3′; K104Stp 5′-ATTGCG GCCGCTCAGTCGACTTACTTATTCATCTATACAGACACAGTAACA ATC-3′.

6. Amplification of CD48 gene.
5′-CACAGATCTAGAACTAGTGCCACCATGTGCTCCAGAGGT TGG-3′; 5′-CACGCGGCCGCAGAGTCGACTCAATCAATCAGGTAA GTAACAGG-3′.

7. Amplification of probe for K18 read-through transcripts.
5′-AATAGATCTAACACTAGTACATAAGGGAACTCAGAGGCT GGC-3′; 5′-AATGCGGCCGCTCAGTCGACATATCCAGTAATGGCA ATGCTGGCTATG-3′.

8. Amplification of probe for 6-16 transcripts.
5′-CggAgATCTCACACTAgTCCAgATgggTTCTCACTATATTg-3′; 5′-TTAgCggCCgCTCAgTCgACATATTgggAATgggggTgTgTgg-3′.

9. Amplification of 3′ K18 LTR for typing.
K18LTR3 5′-GACAGATCTCACACTAGTGCTACAGTGACATCGAG AACG-3′;
K18FLR 5′-ATTGCGGCCGCTCAGTCGACCCCAAACCTTTAAATA TTGTCTCATG-3′.

Analysis of SAg Expression

Total RNA was extracted from 2–10 × 10⁷ PBL and 3–10 × 10⁶ cell lines. For hybridizations, 15–50 μg total RNA was used. Quantification was performed with PhosphorImager (Molecular Dynamics).

Ribonuclease protection assays and the probes protecting a 161 bp human TBP fragment and a 224 bp HLA-A fragment were described (Reith et al., 1994; Bontron et al., 1997). The other riboprobes were as follows. The K18 SAg probe spanned the coding region from nt 162–462. Transcripts were generated with T3 RNA polymerase, after linearization with AvrII. The undigested probe was 351, the protected K18 fragment 299, and the protected K108 and K104 fragments were ~220 nt. The K18 read-through probe was generated by PCR on genomic DNA. Transcripts were generated with T3, after linearization with SpeI. The undigested probe was 365 nt and the protected fragment 325 nt. The CD48 probe was generated by PCR on cDNA. Transcripts were generated with T3, after linearization with SexA1. The undigested probe was 288 nt, the protected fragment 254 nt. The 6-16 probe was generated by PCR on genomic DNA. Transcripts were generated with T3, after linearization with SpeI. The undigested probe was 372 nt, the protected unspliced fragment 309 nt, and the protected spliced fragment was 254 nt.

SAg Assays

Blast assay. PBL were obtained from the Geneva blood bank. IFN-α was from C. Weissmann (IFN-α_1/α_2) and Roche (IFN-α_{2a}, Roferon-A); and IFN-β was from Serono (Rebif); IFN-γ was from Gibco-BRL. They were used at 10-2 × 10^3 U/ml and at 10^3 U/ml if not stated otherwise. LPS was used at 10 μg/ml (Salmonella abortus equi, Sigma). After induction, PBL were irradiated at 3000 rad, washed, and added back to syngeneic T cells at 1:1 ratios. After 2 $\frac{1}{2}$ days of culture, IL-2 was added for the last 24 hr at 10 U/ml. The percentage of blasts in the CD3$^+$ T cell population was determined by FACS by collecting >5 × 10^4 events. Dead cells were excluded and Fc receptors were blocked.

SAg assay with CD69 expression on bulk T cells. 10^6 PBL/ml were incubated for 15 min at 37°C, treated with 10^3 U IFN-$\alpha_{1/2}$ for 1 hr at 37°C, washed 3×, and irradiated at 3000 rad. APCs and T cells were cultured in 96-well plates in a final volume of 200 μl at the indicated ratios for 24 hr at 37°C. CD69 expression was analyzed on CD3$^+$Vβ^+ T cells and T cell blasts by FACS. 2–5 × 10^5 events were collected.

SAg assay with Vβ7 T cells. CD4$^+$ Vβ7 T cells were derived from a SAg responsive donor by repeated cycles of stimulation with Vβ7 antibody 3G5 (Coulter) and syngeneic feeders. 1–5 × 10^5 A20 transfectants were incubated with 10^5 Vβ7 T cells and 10^5 irradiated syngeneic PBL as feeders in 96-well plates. After 48 hr, ^{3}H-Thymidine was added for 18 hr and incorporation measured.

SAg assay with purified primary B cells. B cells were enriched from 10^7 PBL by negative selection. B cells were treated with IFN-α_{2a} (2 × 10^3 U/ml, Roferon-A, Roche) for 1.5 hr or left untreated and induced or not with PMA for 1.5 hr at 37°C (10 ng/ml, Calbiochem). γ-irradiated B cells (3300 rad) were washed and 10^5 APCs and 10^5 T cells/well were used in proliferation assays. To keep B cells alive, a soluble fusion protein (CD154-CD8) was added as 1:50 dilution of a SF9 cell culture supernatant (R. Noelle, Dartmouth). T cells were pulsed for 12 hr with ^{3}H-Thymidine after 48 hr of culture.

Transfectants. Bicistronic expression cassettes containing enhanced yellow or green fluorescent protein (EYFP/EGFP) as reporters were generated (F.M., submitted). Cells were split 24 hr before electroporation; 10 × 10^6 cells were resuspended in 250 ml RPMI with 10 μl (1 μg/μl) linarized plasmid in TE (pH 8.0), in the presence of 1 μl (1 μg/μl) linearized blasticidin resistance gene (BSD, Invitrogen). Stable integrants were selected for resistance of 10 μg/ml BSD. Bulk transfectants were FACS sorted for EYFP/EGFP fluorescence, cloned by limiting dilution, and maintained for no longer than 30 days in continuous culture at 5 μg/ml BSD. Single clones exhibiting mean fluorescence intensities (MFI) of EYFP/EGFP fluorescence in the range of >5 and <10 were selected and this was critical for SAg function. The bicistronic cassette with EGFP allowed to select for the lowest functional SAg expression levels and was superior to the EYFP reporter (F.M., unpublished data).

Inhibition of SAg activity with polyclonal rabbit antibodies and affinity-purified fractions and immuno-precipitations. N-terminal (N,H$_2$N-VPGPTDDRCPA-CONH$_2$) and C-terminal SAg peptides (C,H$_2$N-CFSYQRSLKFRPKGKT-CONH$_2$) were used to immunize rabbits. Anti-HERV-K *env* Abs and the respective preimmune serum were used at 1:250 and 1:1000 dilutions, monoclonal anti-MHC class II Abs (clone G46-6/L243, Pharmingen) at 20 μl/10^6 cells.

Immuno-precipitations using polyclonal rabbit antisera. A C-terminal 3xHA fusion of the SAg (F.M., unpublished data) was produced in rabbit reticulocyte lysates (Promega). The in vitro produced protein was incubated with the indicated dilutions of preimmune serum, anti-N-, -C-antisera, and with the monoclonal anti-HA antibody (HA.11, BabCO) overnight at 4°C, followed by incubation for 1.5 hr at room temperature with 20 μl ProteinA-sepharose in a volume of 100 μl. The pellet was washed 3× in a 0.6% NP40 buffer, and 1/2 was resuspended in loading buffer and analyzed by SDS-PAGE.

References

Ackrill, A.M., Reid, L.E., Gilbert, C.S., Gewert, D.R., Porter, A.C., Lewin, A.R., Stark, G.R., and Kerr, I.M. (1991). Differential response of the human 6-16 and 9-27 genes to alpha and gamma interferons. Nucleic Acids Res. *19*, 591–598.

Barbulescu, M., Turner, G., Seaman, M.I., Deinard, A.S., Kidd, K.K., and Lenz, J. (1999). Many human endogenous retrovirus K (HERV-K) proviruses are unique to humans. Curr. Biol. *9*, 861–868.

Beales, P.E., and Pozzilli, P. (1999). Caution is required with interferon alpha as a potential treatment for type I diabetes. Diabetologia *42*, 385.

Bontron, S., Ucla, C., Mach, B., and Steimle, V. (1997). Efficient repression of endogenous major histocompatibility complex class II expression through dominant negative CIITA mutants isolated by a functional selection strategy. Mol. Cell. Biol. *17*, 4249–4258.

Chehadeh, W., Kerr-Conte, J., Pattou, F., Alm, G., Lefebvre, J., Wattre, P., and Hober, D. (2000a). Persistent infection of human pancreatic islets by coxsackievirus B is associated with alpha interferon synthesis in beta cells. J. Virol. *74*, 10153–10164.

Chehadeh, W., Weill, J., Vantyghem, M.C., Alm, G., Lefebvre, J., Wattre, P., and Hober, D. (2000b). Increased level of interferon-alpha in blood of patients with insulin-dependent diabetes mellitus: relationship with coxsackievirus B infection. J. Infect. Dis. *181*, 1929–1939.

Conrad, B., Weidmann, E., Trucco, G., Rudert, W.A., Behboo, R., Ricordi, C., Rodriquez-Rilo, H., Finegold, D., and Trucco, M. (1994). Evidence for superantigen involvement in insulin-dependent diabetes mellitus aetiology. Nature *371*, 351–355.

Conrad, B., Weissmahr, R.N., Boni, J., Arcari, R., Schupbach, J., and Mach, B. (1997). A human endogenous retroviral superantigen as candidate autoimmune gene in type I diabetes. Cell *90*, 303–313.

Der, S.D., Zhou, A., Williams, B.R., and Silverman, R.H. (1998). Identification of genes differentially regulated by interferon alpha, beta, or gamma using oligonucleotide arrays. Proc. Natl. Acad. Sci. USA *95*, 15623–15628.

Fleischer, B., Gerardy-Schahn, R., Metzroth, B., Carrel, S., Gerlach, D., and Kohler, W. (1991). An evolutionary conserved mechanism of T cell activation by microbial toxins. Evidence for different affinities of T cell receptor-toxin interaction. J. Immunol. *146*, 11–17.

Foulis, A.K., Farquharson, M.A., and Meager, A. (1987). Immunoreactive alpha-interferon in insulin-secreting beta cells in type 1 diabetes mellitus. Lancet *2*, 1423–1427.

Goff, S.P. (1996). Operating under a Gag order: a block against incoming virus by the Fv1 gene. Cell 86, 691–693.

Hakem, R., Le Bouteiller, P., Jezo-Bremond, A., Harper, K., Campese, D., and Lemonnier, F.A. (1991). Differential regulation of HLA-A3 and HLA-B7 MHC class I genes by IFN is due to two nucleotide differences in their IFN response sequences. J. Immunol. 147, 2384–2390.

Hanninen, A., Jalkanen, S., Salmi, M., Toikkanen, S., Nikolakaros, G., and Simell, O. (1992). Macrophages, T cell receptor usage, and endothelial cell activation in the pancreas at the onset of insulin-dependent diabetes mellitus. J. Clin. Invest 90, 1901–1910.

Hasuike, S., Miura, K., Miyoshi, O., Miyamoto, T., Niikawa, N., Jinno, Y., and Ishikawa, M. (1999). Isolation and localization of an IDDMK1,2-22-related human endogenous retroviral gene, and identification of a CA repeat marker at its locus. J. Hum. Genet. 44, 343–347.

Held, W., Waanders, G.A., Shakhov, A.N., Scarpellino, L., Acha-Orbea, H., and MacDonald, H.R. (1993). Superantigen-induced immune stimulation amplifies mouse mammary tumor virus infection and allows virus transmission. Cell 74, 529–540.

Herman, A., Croteau, G., Sekaly, R.P., Kappler, J., and Marrack, P. (1990). HLA-DR alleles differ in their ability to present staphylococcal enterotoxins to T cells. J. Exp. Med. 172, 709–717.

Kappler, J., Kotzin, B., Herron, L., Gelfand, E.W., Bigler, R.D., Boylston, A., Carrel, S., Posnett, D.N., Choi, Y., and Marrack, P. (1989). V beta-specific stimulation of human T cells by staphylococcal toxins. Science 244, 811–813.

Le Page, C., Genin, P., Baines, M.G., and Hiscott, J. (2000). Interferon activation and innate immunity. Rev. Immunogenet. 2, 374–386.

Levy, D.E., Lew, D.J., Decker, T., Kessler, D.S., and Darnell, J.E.J. (1990). Synergistic interaction between interferon-alpha and interferon-gamma through induced synthesis of one subunit of the transcription factor ISGF3. EMBO J. 9, 1105–1111.

Luppi, P., Zanone, M.M., Hyoty, H., Rudert, W.A., Haluszczak, C., Alexander, A.M., Bertera, S., Becker, D., and Trucco, M. (2000). Restricted TCR V beta gene expression and enterovirus infection in type I diabetes: a pilot study. Diabetologia 43, 1484–1497.

Marrack, P., Winslow, G.M., Choi, Y., Scherer, M., Pullen, A., White, J., and Kappler, J.W. (1993). The bacterial and mouse mammary tumor virus superantigens; two different families of proteins with the same functions. Immunol. Rev. 131, 79–92.

Mein, C.A., Esposito, L., Dunn, M.G., Johnson, G.C., Timms, A.E., Goy, J.V., Smith, A.N., Sebag-Montefiore, L., Merriman, M.E., Wilson, A.J., et al. (1998). A search for type 1 diabetes susceptibility genes in families from the United Kingdom. Nat. Genet. 19, 297–300.

Pelegrin, M., Devedjian, J.C., Costa, C., Visa, J., Solanes, G., Pujol, A., Asins, G., Valera, A., and Bosch, F. (1998). Evidence from transgenic mice that interferon-beta may be involved in the onset of diabetes mellitus. J. Biol. Chem. 273, 12332–12340.

Reith, W., Ucla, C., Barras, E., Gaud, A., Durand, B., Herrero-Sanchez, C., Kobr, M., and Mach, B. (1994). RFX1, a transactivator of hepatitis B virus enhancer I, belongs to a novel family of homodimeric and heterodimeric DNA-binding proteins. Mol. Cell. Biol. 14, 1230–1244.

Simms, P.E., and Ellis, T.M. (1996). Utility of flow cytometric detection of CD69 expression as a rapid method for determining poly- and oligoclonal lymphocyte activation. Clin. Diag. Lab Immunol. 3, 301–304.

Singh, B., Prange, S., and Jevnikar, A.M. (1998). Protective and destructive effects of microbial infection in insulin-dependent diabetes mellitus. Semin. Immunol. 10, 79–86.

Somoza, N., Vargas, F., Roura-Mir, C., Vives-Pi, M., Fernandez-Figueras, M.T., Ariza, A., Gomis, R., Bragado, R., Marti, M., and Jaraquemada, D. (1994). Pancreas in recent onset insulin-dependent diabetes mellitus. Changes in HLA, adhesion molecules and autoantigens, restricted T cell receptor V beta usage, and cytokine profile. J. Immunol. 153, 1360–1377.

Steinman, L. (1995). Escape from "horror autotoxicus": pathogenesis and treatment of autoimmune disease. Cell 80, 7–10.

Stewart, T.A., Hultgren, B., Huang, X., Pitts-Meek, S., Hully, J., and MacLachlan, N.J. (1993). Induction of type I diabetes by interferon-alpha in transgenic mice. Science 260, 1942–1946.

Stoye, J.P., and Coffin, J.M. (2000). A provirus put to work. Nature 403, 715–717.

Subramanyam, M., McLellan, B., Labrecque, N., Sekaly, R.P., and Huber, B.T. (1993). Presentation of the Mls-1 superantigen by human HLA class II molecules to murine T cells. J. Immunol. 151, 2538–2545.

Sutkowski, N., Conrad, B., Thorley-Lawson, D.A., and Huber, B.A. (2001). Epstein-Barr virus transactivates the human endogenous retrovirus HERV-K18 that encodes a super antigen. Immunity 15, this issue, 579–589.

Tisch, R., and McDevitt, H. (1996). Insulin-dependent diabetes mellitus. Cell 85, 291–297.

Tissot, C., Rebouissou, C., Klein, B., and Mechti, N. (1997). Both human alpha/beta and gamma interferons upregulate the expression of CD48 cell surface molecules. J. Interferon Cytokine. Res. 17, 17–26.

Tonjes, R.R., Czauderna, F., and Kurth, R. (1999). Genome-wide screening, cloning, chromosomal assignment, and expression of full-length human endogenous retrovirus type K. J. Virol. 73, 9187–9195.

Wuarin, J., and Schibler, U. (1994). Physical isolation of nascent RNA chains transcribed by RNA polymerase II: evidence for cotranscriptional splicing. Mol. Cell. Biol. 14, 7219–7225.